

Packet Reception Probability: Packets That You Can't Decode Can Help Keep You Safe

Subham De*, Deepak Vasisht†, Hari Sundaram‡ and Robin Kravets§

Computer Science, University of Illinois at Urbana-Champaign

Email: *de5@illinois.edu, †deepakv@illinois.edu, ‡hs1@illinois.edu, §rhk@illinois.edu

Abstract—This paper provides a robust, scalable Bluetooth Low-Energy (BLE) based indoor localization solution using commodity hardware. While WiFi-based indoor localization has been widely studied, BLE has emerged a key technology for contact-tracing in the current pandemic. To accurately estimate distance using BLE on commercial devices, systems today rely on Receiver Signal Strength Indicator (RSSI) which suffers from sampling bias and multipath effects. We propose a new metric: Packet Reception Probability (PRP) that builds on a counter-intuitive idea that we can exploit packet loss to estimate distance. We localize using a Bayesian-PRP formulation that also incorporates an explicit model of the multipath. To make deployment easy, we do not require any hardware, firmware, or driver-level changes to off-the-shelf devices, and require minimal training. PRP can achieve meter level accuracy with just 6 devices with known locations and 12 training locations. We show that fusing PRP with RSSI is beneficial at short distances (≤ 2 m). Beyond ≥ 2 m, fusion is worse than PRP, as RSSI becomes effectively de-correlated with distance. Robust location accuracy at all distances and ease of deployment with PRP can help enable wide range indoor localization solutions using BLE.



1 INTRODUCTION

Indoor positioning is a widely studied problem in academia and industry [48, 47, 24, 28, 57, 14, 44]. Coupled with the high penetration of consumer radio devices (e.g. smartphones), indoor positioning can re-imagine use of indoor spaces like retail spaces, malls, museums, and warehouses. Today, the contact-tracing challenge due to the pandemic has put an urgent, renewed focus on developing a robust, low-cost, scalable, indoor localization solution. Indoor-localization based contact-tracing¹ that helps us determine if a pair of individuals are “social-distancing,” separated by more than 6ft, may safely re-open the world economy.

Technological solutions for contact tracing that use smartphones are an important complement to normative (e.g., wearing a mask) and policy (e.g. stay-at-home) interventions for mitigating effects of the pandemic. Bluetooth Low-Energy (BLE) is emerging as the key contact-tracing technology and is being used in contact-tracing apps around the world. For example, the Aarogya Setu contact-tracing app² in India, uses BLE and has been downloaded 120M times. The open-source, privacy-preserving contact-tracing framework, BlueTrace³ (deployed in Singapore) uses BLE packets to detect presence (i.e., a smartphone that can hear another must be in proximity of the other.), *not* distance. BLE is preferable to WiFi for contact-tracing: BLE uses $10\times$ less power than does WiFi; BLE can be easily used to infer the presence of nearby peers without presence of WiFi infrastructure. The newly proposed Exposure Notification Service by Apple-Google⁴ also relies on BLE beacons and signal strength measurements.

1.1 Overcoming Key Technological Limitations for Contact Tracing

In this paper, we ask: *Can we develop robust Bluetooth based contact tracing, with existing measurements, deployed on low-cost commodity hardware?* To do so, we need to overcome four fundamental limitations—deployability, bias in RSSI, high packet loss in Bluetooth and multipath effect.

Deployability on commercial smartphones: Bluetooth Low-Energy based apps for contact-tracing have two well-known shortcomings. These apps primarily use either RSSI (Received Signal Strength Indicator) or presence to determine risk to COVID exposure. Prior work [3, 16, 58] demonstrates that RSSI-based methods experience large errors (order of several meters) in positioning, especially in the low RSSI-large distance regime. RSSI has an important benefit: it is present on all modern devices. In contrast, we cannot use CSI (Channel State Information) [24, 53, 48], a recent method that enables sub-meter accuracy, since off-the-shelf devices typically do not report CSI. A recent work [40] has enabled CSI for WiFi in some smartphones, but cannot be applied for BLE. Some contact-tracing apps also use ‘presence’—if one device can hear another—to determine if an individual is close to another infected person. Presence is a poor proxy for distance since devices can hear Bluetooth beacons well beyond 6 ft social distancing radius, and also hear them across aisles and walls.

Biased RSSI Estimates due to Packet Loss: We explain with a conceptual example in Figure 1(a) that shows a Normally distributed RSSI at the receiver, for a fixed transmitter and receiver. In free space, with increasing distance between the transmitter and the receiver, the RSSI distribution shifts to the left, implying a decreasing RSSI at the receiver. RSSI-based methods [3, 30] empirically measure RSSI and use the mean RSSI estimate to infer distance. However, as the distance

1. Contact-tracing requires us to calculate relative distance between individuals. Inferring relative distance from location is straightforward.

2. <https://www.mygov.in/aarogya-setu-app/>

3. <https://bluetrace.io>

4. <https://www.apple.com/covid19/contacttracing/>

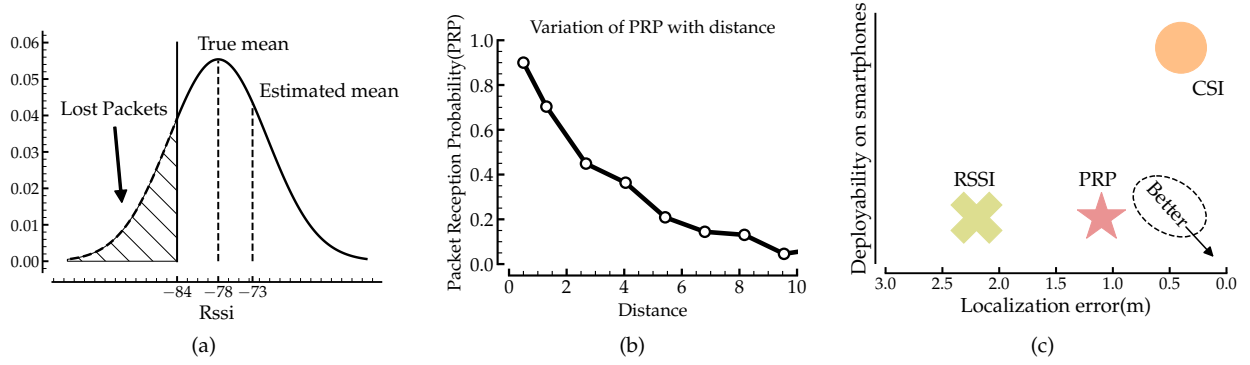


Fig. 1: (a) As the mean RSSI decreases, the error in the RSSI estimate increases because of lost packets. (b) Packet reception in Line-of-Sight (LOS) with -20db transmission power decreases with distance. (c) Packet Reception Probability (PRP) technique is more accurate than RSSI [3, 16, 58] and readily deployable on commercial devices than CSI [24, 53, 48].

between the transmitter and the receiver increases (i.e., the RSSI distribution shifts to the left), packet loss increases with almost certain packet loss at the low-RSSI decoding threshold. Since devices only report RSSI for successfully decoded packets, RSSI-based distance methods suffer from a sampling bias: they use RSSI from decoded packets only. Since they cannot know RSSI values of packets they cannot decode, these methods introduce systematic error in their mean RSSI estimates. This error increases with distance, so much so that at large distances (few meters for BLE), as we shall show in this paper, the mean RSSI estimate becomes de-correlated with distance and is an unreliable indicator. The error is different from the typical reduction in SNR due to increase in distance. The error stems from a sampling bias fundamental to RSSI measurements.

Packet Losses are higher in BLE: Packet loss is a fundamental problem in a low-power protocol like Bluetooth Low Energy. At distances as small as 1 m, in line of sight, around 10% of the packets get dropped in our empirical evaluation, as shown in Figure 1(b). Packet loss rate increases to 50% at 3 m. Thus, the sampling bias in RSSI measurements is a more significant challenge for BLE compared to high-power WiFi protocol based RSSI methods [3, 57, 10]. As pointed out in [7], BLE limits transmission power to reduce energy consumption. BLE v4.0, v4.1, and v4.2 defined maximum output power is 10mW, which is $10\times$ lower than WiFi.

Multipath Effects: Multi-path effects [51, 58] are the second large contributor to RSSI errors. Specifically, the error arises due to reflections of the radio signals by objects in the environment. Thus, the signals from the transmitter travel along multiple paths and combine at the receiver. This combination can be constructive (i.e., in-phase) and increase RSSI or destructive (i.e., out of phase) and reduce RSSI. Since this combination is a function of the environment and *not* the distance between the devices, multipath introduces error in distance measurements.

1.2 A Counter-Intuitive Approach: Exploit Packet Loss to infer Distance

In this paper, we ask a counter-intuitive question: *Could the loss of a packet be a clue to the distance between the transmitter*

and receiver? Intuitively, as the distance between transmitter and receiver increases, the ability to successfully receive packet decreases. In this paper, we build on this intuition to develop a new metric: Packet Reception Probability (PRP), which measures the probability that a receiver successfully receives packets from the transmitter. A simple experiment validates our intuition that PRP can encode distance. We collected packets from BLE beacons transmitting at -20db power at increasing distance values between 1 m to 10 m in a line-of-sight (LOS) scenario. We use maximum likelihood estimates for PRP. We plot the PRP estimate as a function of distance in Figure 1(b). Notice that Figure 1(b) shows that the probability of receiving a packet *decreases* with distance, implying that PRP encodes distance. We show in this paper, that for low energy protocols including BLE, PRP is a good indicator of the distance between communicating devices.

Our approach, Bayesian Packet Reception Probability (B-PRP), is suitable for public spaces including retail stores or libraries, places that are important to current social distancing and contact tracing efforts. B-PRP is a PRP-based approach that develops a novel Bayesian framework to explicitly model multipath reflections in the environment and deliver robust and accurate localization. The Bayesian framework helps to minimize system deployment costs. A public environment like a retail store contains obstructing materials in the form of stacks or shelves. The shelves (including the items placed on them) absorb or reflect the radio signals directed at them. This leads to a lower packet reception probability at the receiver. At a fixed distance, the packet reception probability will vary based on the number and type of obstacles in the signal path. B-PRP must tease apart the effects of distance from the interference effects of the obstacles, when estimating distance. We observe that we can model public spaces including retail stores in a modular manner comprising open spaces separated by stacks. We explicitly capture the effect of such stacks by modeling the packet reception in absence of stacks and in presence of one stack, two stacks and so on. While we use stacks to model retail spaces, we believe that the abstraction of modeling a geometric element is general enough to apply to other large indoor spaces like libraries, warehouses, factories, etc.

Finally, we present a method to estimate inter-device distance using our approach, a primitive essential to contact-tracing. We evaluated B-PRP in two real-world public places, an academic library setting and in a real-world retail store, and demonstrate the efficacy of our techniques. In both cases, we did not control for human traffic. Our main results:

Localization Accuracy: B-PRP achieves a median localization error of 1.03 m (library) and 1.45 m (retail store). The state of the art Bayesian RSSI system [30] has errors of 1.30 m (library, 26.2% more error) and 2.05 m (retail store, 41.3% more error) when trained with the same number of data points and packets per data point.

Distance estimation for contact tracing: Our contact tracing distance estimation achieves median error of 0.97 m (library) and 1.22 m (retail store) with PRP values. The errors with RSSI are 1.69 m (library, 74.2% more error) and 1.25 m (retail store, 2.4% more error). Using the covid risk metric [46], we see that PRP does 1000X better than RSSI in the library.

B-PRP+RSSI Fusion: Fusion of B-PRP and RSSI modestly improves the overall localization accuracy over B-PRP (Table 2). We see best fusion results at small distances (≤ 2 m). At larger distances (≥ 2 m), errors in RSSI cause fusion results to be significantly worse than B-PRP. PRP+RSSI also improves contact tracing accuracy by 6% for both library and retail store.

Robustness to Multipath: Our multipath model increases the accuracy for PRP from 1.41 m to 1.03 m in the library (a 26.9% improvement) and from 1.60 m to 1.45 m (a 9.3% improvement) in the retail store.

Number of Beacons: As beacon density decreases, B-PRP error is always within 2m while RSSI errors are higher than 3m. With five beacons, B-PRP performs 65% better in library and 50% better in the retail store.

Low Training Overhead: B-PRP can leverage unknown training data to train the B-PRP model, thereby reducing the deployment effort. Specifically, B-PRP can achieve 1.08 m median accuracy with just 8 labelled data points and 4 unlabelled data points.

For completeness, we note that the core limitation of a localization method like B-PRP, a limitation shared with methods including [9, 27, 12, 28] is that it needs deployment of beacons in the public space to locate individuals. However, BLE beacons are inexpensive, and our method, B-PRP, provides meter-level accuracy. A peer-to-peer distance estimation is much more general where we will use devices like smartphones for reception and transmission. We believe that this tradeoff between some upfront infrastructure expense (multiple beacons) and increased localization accuracy is worthwhile in highly frequented public spaces.

2 CONTRIBUTIONS

Our paper makes the following contributions:

Use of Negative Information: To the best of our knowledge, we are the first to build an indoor positioning system that can extract information from *absence of packets*. In contrast, state of the art RSSI based techniques [3, 57, 10], use observed RSSI to infer distance. We accomplish this through a Bayesian formulation of the packet reception probability, a metric that we show encodes distance. We

develop generic stacking models of reception to address multipath effects. While we use PRP as a sole indicator of distance to highlight its benefits, we show that B-PRP when combined with RSSI, improves the performance of the system at shorter distances. Our finding shows how to use BLE to robustly estimate indoor distances, thus opening the door to reliable BLE based contact-tracing that incorporates distance.

Distance estimation for contact tracing without localization:

We directly estimate distance between two individuals *without localization* by exploiting the well-known triangle inequality constraints in Euclidean geometry. In contrast, we may consider estimating contact tracing distance through localization: that is, we first, estimate locations of two persons independently and then calculate the Euclidean distance between the two locations. This approach is sub-optimal—we are estimating location while we are only interested in distance. Also, if we have localization errors for a particular individual, these errors will impact *all* the distance estimations between this individual and other nearby persons. We extend out Bayesian framework to independently estimate distances between pairs of individuals. With the known beacons, we form triangles and we impose triangle inequalities on these distances to rule out many distance configurations in the real world. We improve our distance estimates by $\sim 10\%$ by triangle inequality distance estimation.

Sampling Bias in RSSI: We show the effect of packet loss on the mean RSSI measurements. Furthermore, we show that with increasing distance, mean RSSI becomes highly unreliable due to sampling bias. Our finding is significant because the state of the art RSSI based techniques [3, 57, 10] when applied to BLE, a low-power protocol, are highly unreliable in the 2 m to 6 m range (Table 2). We highlight that 2 m \approx 6 ft, the social distancing range.

Readily Deployable Solution: Our B-PRP framework does not require any hardware, firmware, or driver-level changes in off-the-shelf devices, and requires minimal deployment and re-training costs. In contrast, CSI [24, 53, 48], which can deliver sub-meter accuracy, requires firmware or hardware changes. This is significant: due to the simplicity of the packet reception framework, we can immediately deploy B-PRP as an application on off-the-shelf commodity smartphones.

3 MOTIVATION

In this work, we focus on localizing individuals in indoor public spaces like retail stores, libraries. In these spaces, indoor positioning using BLE beacons can enable traditional applications like capturing behavioral data about shoppers, as well as novel applications like enforcing social distancing and contact-tracing. BLE offers an unique advantage for localization. Due to its low power budget, it can be turned on frequently and hence, enable more frequent location updates as compared to high power protocols like Wi-Fi. Recall that BLE’s maximum transmit power (10 dBm) is 10 times lower than that of Wi-Fi (20 dBm). This factor, in addition with its ubiquitous presence on off-the-shelf smartphones, has made BLE the natural choice for such applications.

Traditional BLE localization techniques either use RSSI (Received Signal Strength Indicator) [3, 16, 58] or CSI (Channel State Information) [24, 2]. CSI for BLE is not available on commercial devices like smartphones. On the other hand, RSSI measurements are noisy due to packet loss and multi-path effect. While multi-path effects [51, 58] are well-documented, let's dig deeper into the challenge of packet loss.

First, we identify that packet losses can be mainly attributed to two reasons—random errors and low signal strength. Errors can occur uniformly at random irrespective of the RSSI of the packet. As a result, such errors do not introduce any bias in the aggregate estimate of RSSI. On the other hand, all packets that are received with a signal strength below a certain decoding threshold get dropped. Since we cannot observe the RSSI values of these low RSSI packets, and hence cannot include them in our aggregate estimates, we should expect to see a positive bias introduced in our RSSI measurements.

Let's mathematically validate our hypothesis of positive bias in RSSI aggregate estimates. Let us assume that the actual RSSI values at a certain location follow the Gaussian distribution $\mathcal{N}(\mu, \sigma^2)$. Let's further assume that the RSSI decoding threshold is α . Since we drop all packets below the threshold, our aggregate RSSI estimates will be based on a Normal distribution truncated at α . The new mean of this truncated normal distribution is given by

$$\hat{\mu} = \mu + \frac{\phi(\alpha)}{1 - \Phi(\alpha)} \sigma, \quad (1)$$

where, $\phi(\alpha)$ is the pdf of normal distribution evaluated at α , $\phi(\alpha) \geq 0$. $\Phi(\alpha)$ is the cdf value of the normal distribution at α , $\Phi(\alpha) < 1$. Thus the estimate $\hat{\mu}$ that we obtain by measuring received RSSI values is biased by a positive amount of $\frac{\phi(\alpha)\sigma}{1-\Phi(\alpha)}$. As we move towards the lower RSSI regime, μ becomes closer to α . As a result, both $\phi(\alpha)$ and $\Phi(\alpha)$ increases with lower RSSI values, which leads to a higher bias in the estimated mean RSSI.

Note that we cannot trivially estimate μ from $\hat{\mu}$ in Equation (1) since in practice, multi-path effects alter the values of the RSSI in the received packets. Thus recovering μ, σ using say Maximum Likelihood Estimates by assuming a value of α is non-trivial.

Based on the above discussion, we identify that our solution requires three important properties—eliminating positive bias due to packet loss, robustness to multi-path effects, and ease of deployability on commercial devices. CSI meets the first two properties but misses the important requirement of deployability. RSSI is deployable, but has positive bias and is sensitive to multi-path.

4 SYSTEM DESIGN

In this paper, we solve the challenges with RSSI by asking a different question—*Can we use the loss of packets as a signature itself to measure distance?* We define a random variable, packet reception probability, $prp(b)$, for a beacon b whose expected value is defined as:

$$\mathbb{E}(prp(b)) = \frac{\sum_i \mathbf{1}_{i=b}}{R(t_l - t_f)} \quad (2)$$

Here, $\mathbf{1}$ is the indicator function that is 1 if and only if packet i is received from beacon b , R is the sending rate of the beacon, and where t_l and t_f are the timestamps of the last and the first packet received from beacon b . Notice that the right hand side of Equation (2) is just the frequentist estimate of the probability of packet reception from beacon b : number of packets received divided by the total number of packets sent by beacon b .

One might wonder if PRP provides additional information beyond RSSI measurements. Notice that by directly modeling packet reception, we are leveraging absence of information (packet loss). RSSI is measured for packets that are successfully received, but not for dropped packets. Therefore, a system that drops 90% of the packets and 50% of the packets may have the same measured RSSI, but we know one of them has lower true RSSI, and hence is farther off, by looking at the packet reception probability. Also, **packets that are successfully received and influenced by multipath effects, only impact RSSI mean estimate but not expected PRP value $\mathbb{E}(prp(b))$** . Now we will focus on how to use PRP to measure location.

4.1 Estimating Location using PRP

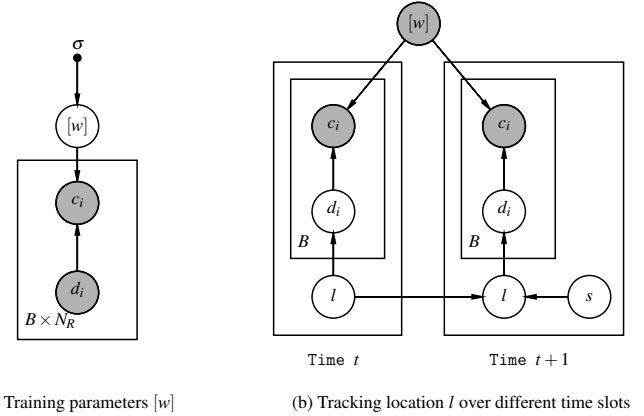


Fig. 2: **Graphical model:** Shaded nodes are observed, while we need to estimate the unshaded ones. We use the data on number of received packets c_i measured from B beacons at N_R reception locations to train the PRP parameters $[w]$. During tracking, we use the trained parameters $[w]$ and $c_{i,t}$ to estimate location l_t .

Recall, in Figure 1(b), PRP degrades with distance. In this section, we discuss how we can model the relationship between PRP and distance, and use this relationship to infer location. Specifically, PRP (prp) depends on three factors: (a) distance (d), (b) sending rate (R), and (c) transmission power (p_t). In this subsection, we model the relationship in free space (Figure 3(A)). We will incorporate the effect of multipath in subsequent sections.

We use a Bayesian model to model the relationship between PRP estimates from multiple beacons and the underlying physical location. Our choice of the Bayesian approach is motivated by two key design benefits: (a) It allows us to infer not just the location, but also quantifies the uncertainty in the location estimate. Such estimates are very helpful when the location is used for higher-layer applications like customer behavior analytics, contact-tracing. (b) It can be extended to scenarios when the beacon

location itself is unknown or the training set is small. As we show in Section 5, this reduces the deployment costs.

We model prp as a function g of the distance d , sending rate R and power p_0 of the beacon. Assume that we receive a packet from beacon (x_b, y_b) at location (x_r, y_r) . We calculate the Euclidean distance d between the beacon and receiver. Then, assuming that we know sending rate R and transmission power p_0 , we can model the number of packets received c received at (x_r, y_r) as drawn from a binomial distribution with parameter prp :

$$\begin{aligned} c &\sim \text{Bin}(N, prp), && \text{binomial distribution,} \\ prp &= g(d, R, p_0), && \text{PRP link function,} \\ d &= \sqrt{(x_b - x_r)^2 + (y_b - y_r)^2}, && \text{distance to beacon } b. \end{aligned}$$

N is the total number of packets sent out by the beacon is proportional to the product of the sending rate R , and the time spent T_r at location r . The function $g(d, R, p_0)$ is a link function that connects the underlying infrastructure parameters (R, p_0) and physical distance d , to the packet reception probability.

In identifying the right representation of g , we need to keep two considerations in mind: (a) the value of g has to be between 0 and 1, and (b) g must encapsulate relationship between d , R and p_0 , not just their direct effect on prp . Therefore, we model $g(d, R, p_0)$ as a logistic function of quadratic interaction between the parameters.

$$\text{logit}\{g(d, R, p_0)\} = w_0 + \sum_i w_i \theta_i + \sum_{i,j} w_{i,j} \theta_i \theta_j \quad (3)$$

where, $\text{logit}(p) = \log(p/1 - p)$. And where, $\theta_1, \theta_2, \theta_3$ correspond to the variables of d, R, p_0 respectively. The coefficients $[w] = [w_i, w_{i,j}]$ are drawn from a non-informative prior $N(0, \sigma)$ —a zero mean Normal distribution with variance σ . We choose σ to be large in our system to allow for a large range of values.

Our Bayesian formulation above is shown in Figure 2(a). Our framework operates as follows:

Training Phase: During training, we use a data set D collected in an environment to estimate the underlying parameters. Specifically, we need to estimate the posterior distribution of the unknown parameters $[w]$ given data D i.e. $P([w] | D)$. The training set, D , comprises BLE logs. Specifically, to obtain D , we stand at N_R locations in our testing area and listen to the packets from B beacons. Assume further, that we know the B beacon locations (x_b, y_b) , $b \in \{1, \dots, B\}$ and N_R reception locations (x_r, y_r) , $r \in \{1, \dots, N_R\}$. We will relax this assumption in Section 5.

Test Phase: During test phase, we do not know the reception locations, (x_r, y_r) $r \in \{1, \dots, N_R\}$. We use the measured prp and the parameters estimated during the training phase to estimate the receiver location. We use PyMC3 [39] framework to do the inference.

Adding Human Mobility: Finally, we note that human location across time is not independent. Rather, locations are constrained by the time between them and the average moving speed of a person. If we wish to track individuals at temporal resolution δ , and if a person reaches a location at time t with speed s_t , we can constrain that location in terms of previous location at $t - 1$

$$s_t \sim U(0, S_{max}), \quad \text{speed,}$$

$$\begin{aligned} x_t | x_{t-1} &\sim \mathcal{N}(0, s_t * \delta), && x_t \text{ constrained by } s_t \times \delta, \\ y_t | y_{t-1} &\sim \mathcal{N}(0, s_t * \delta), && y_t \text{ constrained by } s_t \times \delta. \end{aligned}$$

Where, S_{max} is a constant in our model denoting maximum movement speed of a human (similar to [11]). We estimate speed and location of a person from prp data.

4.2 Combating Multipath Effect

We have assumed a free-space propagation model so far, but real-world environments have obstacles. We observe that the main contributor to multipath effect in public spaces like retail stores (or libraries) are the stacks used to list products (or books) and to separate aisles. In such scenarios, the prp value depends not just on the distance, but also on the number of stacks the signal has to cross. Crossing one stack is easier than crossing two and will cause fewer packet drops.

To build on this observation, we explicitly model the number of stacks in our framework. This allows us to not just estimate the distance between a beacon and a receiver, but also estimate the number of stacks between them. Estimating this geometric information is useful for both: combating multipath, and exploiting in higher-layer applications. For instance, retail store apps need to estimate what aisle a customer is shopping in, contact-tracing apps want to discount for infection spread if customers are close (but across aisles). To estimate the stack separation, we divide the store layout in Figure 3 into five portions based on the given beacon—free space(F-S), one stack (1-S), two stacks away (2-S), corridor (C) and desk (D). In the figure, the packets to receiver 1 in F-S do not have to go through any obstacles. The packets to receiver 2 in 1-S and 3 in 2-S go through one and two interfering stacks respectively. Receiver 4 is in a corridor. We limit ourselves to two stacks away in the model, because we empirically observe that two stacks or more have similar effects on packet reception (high loss).

Then, we parameterize our link function with a variable, γ that denotes the geometric-element separation. We represent the new link function as $g_\gamma(d, R, p_0)$. Now, at training time, we estimate parameters for the functions—free space g_{F-S} , one stack g_{1-S} , two stack g_{2-S} and corridor (C) model g_C . We use a Bayesian training procedure similar to the free-space scenario. We segment our training data into the different scenarios, and use the segment-specific data to learn the parameters in each g_γ . For example, the data with one stack separation is used to train g_{1-S} . During testing, B-PRP uses the maximum likelihood model to identify the underlying location as well as stack separation.

At first blush, it might seem very complex to identify γ for each of the B beacons. We exploit the knowledge of the store geometry and beacon arrangements within the store to significantly reduce the number of unknowns. Assume that beacons a and b are in the same aisle adjacent to each other. Then, *regardless of where the individual is, beacons a and b must have the same model type γ with respect to the receiver*. Similarly, if beacons a and b are in neighboring aisles, and the model type γ is $F - S$ for a , then γ must be $1 - S$ for b . Thus, given a location x_t, y_t , knowledge of store geometry and beacon arrangements help fix the model type for *all* beacons, given the model type for *any one* beacon.

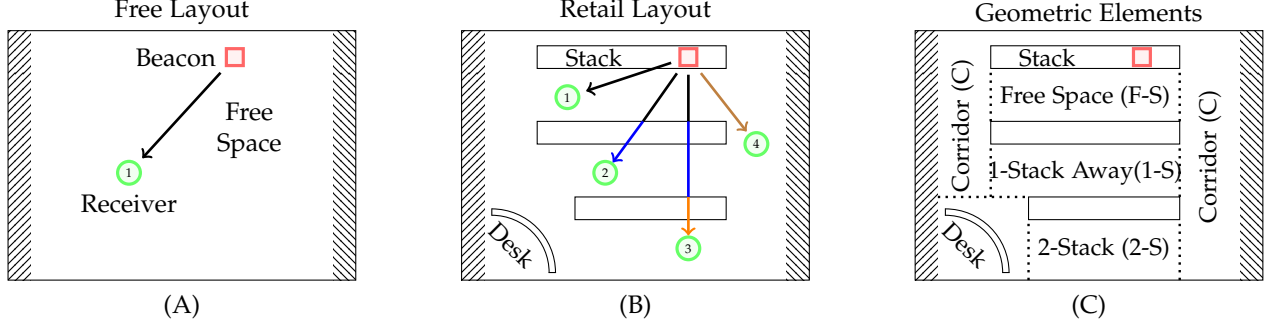


Fig. 3: **Modelling Obstacles and Multipath**: In (A), there is no obstruction in the path of the receiver. In retail layout (B), receiver 1 is in free space with beacon, 2 is one stack away and 3 is two stacks away. 4 is an open region of the layout, i.e. the corridor. We segregate the retail layout in (C) into geometric elements based on the relative position of beacon and receiver.

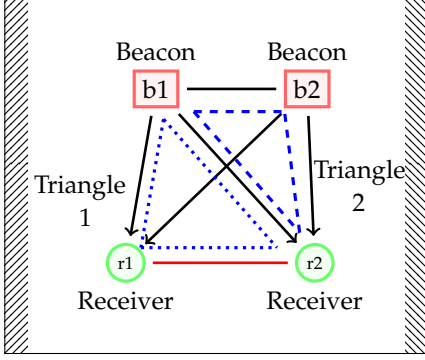


Fig. 4: Modeling contact tracing distance optimizing joint likelihood of observed PRP values and triangle inequalities

4.3 Estimating Distance for Contact Tracing

Given our framework, we could trivially estimate the distance between two individuals using a two-step approach: first, estimate their locations independently and second, calculate the Euclidean distance between the two locations. Then, we could use this distance to ascertain whether two individuals were in contact for contact-tracing. However, this approach is sub-optimal. It requires us to determine four unknowns — (x, y) for the two devices, while we are only concerned about the final distance estimate between the two devices. Also, if we make errors in location estimation for an individual, that impacts all the distance estimations of this individual with other neighboring persons. In other words, we get correlated errors for independent distances between different pairs of individuals. **Can we do better?**

At a high level, we can improve the distance estimation process using two insights. *First*, we don't need to model individual locations if we just care about distance. Therefore, we explicitly incorporate the distance between two devices as part of our Bayesian model. This helps us reduce the number of unknowns in our framework, and also helps to model the distance between each pair of individuals as an independent unknown. *Second*, we leverage the triangle inequality. The triangle inequality states that given a triangle, the sum of two edges has to be greater than or equal to the third edge. This helps us rule out many triangular distance configurations. We present a detailed formulation of these insights below.

Finally, one might wonder: why do we need all this complexity? Why don't we just use the direct transmission between two devices to estimate distance—device A transmits

to device B, device B measures PRP, and we convert that to distance? This approach would create a posterior distribution for distance, but with a large variance because interference by other nearby persons increases the uncertainty in our posterior distance distribution. To shrink this variance, we need other distance measurements, either to known beacons or to many other peers.

In this paper we adopt an infrastructure-assisted approach described above to help compute distances between pairs of individuals. Given that public indoor spaces like retail stores or restaurants (or even businesses) are more likely to be crowded, an infrastructure-assisted approach is reasonable in these settings.

Approach: We explain our approach using a toy example (pictorially represented in Figure 4) which contains two beacons $b1, b2$ and two receivers $r1, r2$. We are interested in finding the distance $d_{r1,r2}$. The latent variables are $(d_{b1,r1}, d_{b1,r2}, d_{b2,r1}, d_{b2,r2})$, on which we have prp data. $d_{b1,b2}$ is known.

First, we infer latent variables $(d_{b1,r1}, d_{b1,r2}, d_{b2,r1}, d_{b2,r2})$ by constructing a joint likelihood function with two components—observed prp values, and triangle inequalities. Taking the receiver $r1$ as an example, we have the triangle $(r1, b1, b2)$ which gives us three triangle inequalities that can be converted to likelihood values as

$$L_T = \log P(d_{r1,b1} + d_{r1,b2} - d_{b1,b2} > 0) \\ + \log P(d_{r1,b1} + d_{b1,b2} - d_{r1,b2} > 0) \\ + \log P(d_{r1,b2} + d_{b1,b2} - d_{r1,b1} > 0) \quad (4)$$

For estimating the latent variables involving the receiver $r1$, we can write down the joint log likelihood function as:

$$\max[\log P(prp_{r1,b1}|d_{r1,b1}) + \log P(prp_{r1,b2}|d_{r1,b2}) + L_T]$$

Second, we infer $d_{r1,r2}$ by maximizing the likelihood of triangle inequalities involving triangles with two receivers and one beacon. We have two triangles $T_1 = (r1, r2, b1)$ and $T_2 = (r1, r2, b2)$. We can construct the likelihood functions for T_1 and T_2 similar to Equation (4). We maximize

$$L = \max_{(d_{r1,r2})} [L_{T_1} + L_{T_2}|d_{b1,r1}, d_{b1,r2}, d_{b2,r1}, d_{b2,r2}].$$

We use PyMC3 potentials to construct these joint likelihood functions and then apply MCMC sampling techniques to solve them. We can also use RSSI or PRP+RSSI instead of PRP in our likelihood functions, which will serve as our different methods in Section 8.3.

5 SYSTEM DEPLOYMENT AND OPTIMIZATION

To summarize, the B-PRP system operates in following steps:

- **Deployment:** We deploy BLE beacons at known locations in an environment like a retail store. The location of the beacons as well as the floor plan is uploaded to a B-PRP server. The server can reside on the cloud or be an edge device local to each environment.
- **Training:** A user walks to fixed locations in the store with a smartphone app or another BLE receiver and measures the PRP values. The PRP values are uploaded to a server. The server uses these labelled PRP values, the beacon locations, and the floor plan to train the B-PRP model.
- **Localization and contact tracing:** Finally, when new users walk in, they measure PRP for beacons already deployed in the store. The app on the smartphone uploads the PRP values to the server. The server uses the trained model to infer location of the users and sends it back to the user. The server also uses the PRP values from multiple users to infer the proximity distance between them. Note that, this system is centered on the user. If the user chooses not to share the PRP values with the server, no location estimation and contact tracing can be performed. Furthermore, the design also conserves power on the smartphone because the user never has to transmit any BLE packets.

Finally, we transmit beacons using BLE advertising mode. This prevents the need for making any explicit connection between the user device and the beacon. The user device can ignore the advertising beacons to avoid localization.

Reducing Deployment Overhead: Deploying the localization infrastructure has two major overheads—setting up the beacons at exact locations, and training. Knowing the location for beacons deployed by a large store is labor intensive. Similarly, training involves standing at multiple known locations inside the layout and collecting data for certain period of time. We ask two questions—1. *Instead of costly human labor, can we infer most beacon locations from training data?* 2. *Can we leverage data from unlabeled locations of store workers to train our model?*

As it turns out, we can affirmatively answer both these questions in our formulation. We can leverage unlabelled data (without location information) that is collected by store workers as they move around the store to help train the model as well as to infer most beacon locations. We use data collected by store workers D to solve both problems. D contains number of packets received from all B beacons at all N_R training locations. Let us assume that we know the locations of a small number $b \ll B$ primary beacons, with the remaining $B - b$ beacon locations unknown; Ideally we will like b to be as close to 0 as possible. Also assume that only a small number $r \ll N_R$ locations are known, with the remaining $N_R - r$ locations unknown. Our goal is to infer $B - b$ beacon and $N_R - r$ training locations from D along with the packet reception model parameters $[w]$.

To enable this, we view the model through a generative process. We initialize the $(B - b)$ beacon and $(N_R - r)$ unknown reception locations from a uniform prior over the testing area which is of dimension $W \times L$. We want to jointly estimate the distribution of the unknown beacon locations $\{l_j\}, j \in \{1, \dots, B - b\}, \{l_k\}, k \in \{1, \dots, N_R - r\}$

and packet reception model parameters $[w]$, given data D . In other words, we want to estimate the posterior distribution $P([l_j, l_k, w] \mid D)$. This can be easily achieved, given the Bayesian nature of our model. We use standard **Markov Chain Monte Carlo (MCMC)** based Bayesian inference techniques to compute the posterior distribution over the unlabelled data points and beacons. We use **No-U-Turn sampling (NUTS)** [17] included with PyMC3 [39] to perform MCMC sampling. Therefore, B-PRP can leverage unlabeled data as well as unlabelled beacon locations to improve its location estimates and reduce the deployment overhead.

6 EXPERIMENTAL SET UP

We evaluate B-PRP in two testbeds—an academic library and a retail store. Both spaces have shelves segregating the floor space into rectangular regions, i.e. aisles and corridors. The two environments differ in three main aspects—difference in layout, i.e. arrangement of rectangular areas and the presence of walls around the space, difference in material of shelves, and human interference. The retail store had more dynamic customer traffic movement during the experiments.

Library: We show the layout of the library space, 14m by 8m, in Figure 5(a). It has three wooden shelves (each 11m long & 0.5m wide). The aisles between two stacks are 0.7m wide. We placed two rows of 12 beacons on each stack. We manually measured each inter-beacon distance. The distance between two adjacent beacons on the same row is 0.91m. The distance between two devices kept opposite each other on the same shelf, but facing two different aisles is 0.43m. We carried out our experiments during regular library hours.

Retail Store: Figure 5(b) shows a retail store with dimensions: 10m by 10m. The environment has four steel stacks (1.27m wide each; three are 7.5m long, one is 6m long). The aisles between two stacks are 1.8m wide. We place two rows of beacons on each stack. The inter-beacon distance on the same row is 1m. Retail store is a challenging environment due to the presence of steel structures as well as worker and customer movement during the experiments.

6.1 Devices

We use following devices for our experiments—Bluvision iBeeks [20], BluFi [6], TI packet sniffer, a laptop and Android smartphones (Nexus5x, NuuA4L). iBeeks or iBeacons are battery operated BLE beacons. They support a wide range of broadcasting power from -40dBm to $+5\text{dBm}$. -40dBm translates to 3m line of sight range, while $+5\text{dBm}$ gives us a range of 150m. For our experiments, the beacons send 10 packets per second at -15 dBm power. We deploy 60 iBeacons in the library and 38 beacons in the retail store.

We use three receiver devices for BLE: Texas Instrument Packet Sniffer (CC2540 dongle), Nexus 5X smartphone, NuuA4L smartphone. iBeacons broadcast BLE packets in three channels— 37, 38 and 39. The sniffer can filter out packets from specific channels. We connect the sniffer to a Windows laptop and use it for packet reception from beacons. For the Android phones, we built an android app using Altbeacon [1] library to scan BLE channels.

6.2 Baselines

We compare B-PRP against state-of-the-art in RSSI-based positioning:



Fig. 5: **Experimental Testbed:** We conduct our experiments in a library (a) and a retail store (b) using devices shown in (c)—Beacon, Blufi, Sniffer, Laptop, Nexus5X and NuuA4L android smartphone.

- **Horus** [57] is an RSSI fingerprinting technique that was originally tested with WiFi. We extend it to BLE. For fairness, we use Horus with the same number of training locations as other baselines—12 for library and 9 for retail store. The inter-state distance is $3.5m$ for library and $1.85m$ for retail store.
- **Bayesian RSSI** [30] uses a generative model based on RSSI to determine location. We set the priors and parameter values following recommendations in [30].
- **Bayesian RSSI Fingerprinting** (or Bayesian FP) [8] is a Bayesian Fusion technique applied to a fingerprinting based method for BLE devices. It stores fingerprints like Horus, but employs fusion technique to combine current RSSI and prior location information.
- **MCL** [18] is a range-free localization technique and uses proximity rather than ranging information to localize nodes. It observes whether a packet was received from a device and infers whether the reception location is inside or outside a threshold distance from the beacon.

To ensure fair comparison, we use the same training data across all techniques. Furthermore, for RSSI based techniques, we use mean RSSI values over all packets used by the PRP technique. That is, **if PRP uses k packets at a location, we use the mean RSSI value over the same k packets.** This removes inter-packet RSSI variance at the same location, *improving* RSSI localization. RSSI results are significantly worse without averaging.

There is more recent work in CSI-based positioning [24, 53, 47], but CSI data is not available on most commercial smartphones. Hence, we do not cover these baselines. For reference, the state-of-the-art CSI-based method achieves a median localization error of 86 cm[2]. However, this work requires CSI data on phones and multi-antenna beacons, both of which are not mainstream yet, and hence, cannot be deployed at scale for applications like contact tracing.

6.3 Data Collection

We collected data for both layouts in two phases—training and localization. We collected data at stationary spots to train B-PRP and competing baselines. We marked some fixed places for each layout and stood there for 1 minute to receive data from the beacons. We used 12 such spots for the library layout and 9 locations for the retail store layout.

We collected data in both test-beds to compare the accuracy of localization and contact tracing techniques. To track and test on data from a moving person, we asked users to naturally move inside the layout with the laptop and sniffer in hand. We used fixed movement paths and marked spots along the path. Each path or trace is a simulated

movement carried out in real time between such marked spots. We stop at each marked place for 10 seconds, and we move at a normal walking speed of $0.5m/sec$ between the spots. We can now calculate the ground truth location at any time within the movement trace. Please note that **we evaluate our location estimates throughout the movement trajectory.** They are not restricted to the marked fixed spots.

7 MICRO BENCHMARK

We present microbenchmarks to better understand PRP:

Relationship to RSSI: First we ask how PRP varies with RSSI and if packet reception is directly dependent on RSSI. We plot this relationship in Figure 6. As seen in the figure, there is an expected trend between the two parameters, but there is also significant variance for each value of PRP. This implies that the relationship between packet reception and RSSI is not determined by a hard threshold, but is instead more probabilistic. The probability of packet reception goes down with RSSI but several other factors including random noise come into play.

Translation across devices: Does the relationship of PRP with distance depend on a device? To answer, we collect PRP values at the same location with two android smartphones: Nexus5X and NuuA4L. As shown in Figure 6, we see very close trends in PRP vs distance with minor variations⁵.

Robustness to interference: Does interference from other in-band transmissions like WiFi hurt PRP? To understand this, we conduct the following experiment. We setup a WiFi router on 2.4GHz WiFi band and use two laptops to saturate the link using the iperf utility[21]. We measure the PRP-distance relationship with WiFi interference turned on and off. We see negligible variation in the relationship between PRP and distance (Figure 6(right)). This is because the three advertising channels of BLE fall between or outside the main frequencies used for IEEE 802.11, allowing for better coexistence with WiFi.

Does interference from many co-located beacons hurt PRP? BLE beacons send out short advertising messages in passive mode containing a payload of at most 31 bytes. As pointed out in [13], the small size of the advertising messages helps in avoiding any significant collisions of upto 200 or more co-located devices. Similarly, the co-location of many receivers or scanning devices will not impact PRP. In our setup, the receiver receives the advertising message in a passive scanning mode, and does not respond in any way. As a result, many scanning devices do not lead to any interference.

5. The experiments were conducted on different days for each smartphone

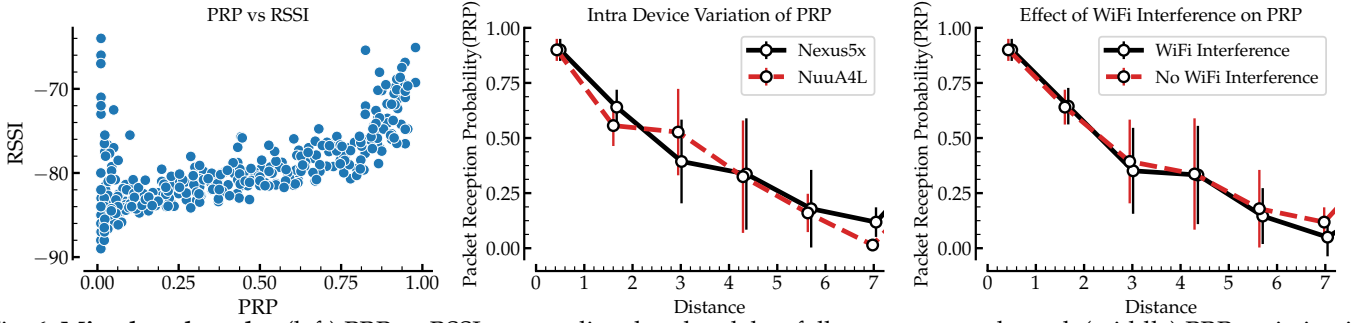


Fig. 6: **Microbenchmarks:** (left) PRP vs RSSI are not directly related, but follow an expected trend. (middle) PRP variation is similar across two different android devices—Nexus5X and NuuA4L. (right) PRP is robust to ambient WiFi interference.

8 RESULTS

We compare the localization performance of baselines against B-PRP in Section 8.1. For these results, we assume that all beacon and reception locations are known (for all methods). In Section 8.2, we evaluate the robustness to the number and placement of beacons. In Section 8.3, we evaluate the contact tracing performance of the PRP against RSSI. In Section 8.4 and Section 8.5, we list the results for B-PRP when we reduce the beacon set-up costs and the number of labelled training locations. In summary:

- Median error for B-PRP is 1.03m and 1.45m in library and retail store. The corresponding errors for the best baseline, Bayesian RSSI are 1.3m and 2.05m.
- Median error for contact tracing distance estimation with PRP is 0.97m and 1.22m in library and retail store. The corresponding errors with RSSI are 1.69m and 1.25m.
- B-PRP is more robust than RSSI to decreasing number of beacons. With 5 beacons, B-PRP performance is 65% better in the library and 50% better in the retail store.
- B-PRP performs better than Bayesian RSSI when we use only Non Line-of-Sight(NLOS) or far away beacons. With beacons placed greater than 6m distance, B-PRP gives error of 1.53m and 2.07m in LOS and NLOS. RSSI errors are 3.85m and 5.15m.
- B-PRP can reduce set-up cost by learning most beacon locations. Given data from 12 training locations, B-PRP needs to know exact location of only 6 beacons and it can infer the remaining 54 beacon locations while giving an accuracy of 1.05m.
- B-PRP can reduce retraining efforts by leveraging data from unknown locations. Having data from 12 known locations vs (6 known + 6 unknown) locations gives the same accuracy level. We can improve accuracy $\sim 40\%$ by adding data from unlabeled spots.

8.1 Localization Accuracy Evaluation

We compare the accuracy of B-PRP against baselines. We use Euclidean distance to measure the error between actual and estimated locations for each time window. We show

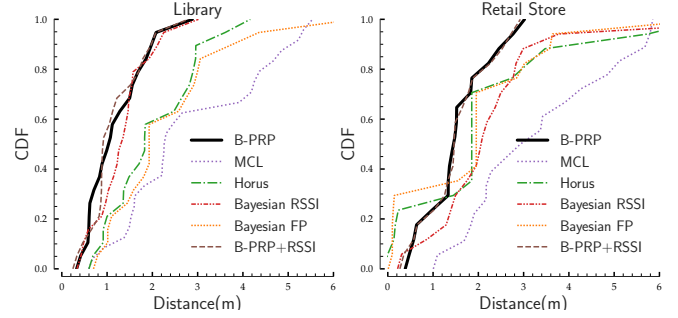


Fig. 7: **CDF error distribution** for Bayesian PRP and baselines in library and retail store. For RSSI techniques, we have averaged RSSI value across the same number of packets that was used by PRP technique.

cumulative distribution over errors in Figure 7 and median error in Table 1.

First, observe that B-PRP achieves a median error of 1.03m and 1.45m in the library and retail store. The next best method, Bayesian RSSI, achieves errors of 1.3m and 2.05m. The errors for all methods are higher for the retail store which has more human traffic than the library. B-PRP can outperform baselines due to two reasons: (a) B-PRP can extract information even from lost packets, and (b) It incorporates a new multipath-model that can work in the presence of obstacles. The stack model helps to increase the median accuracy of B-PRP from 1.41m to 1.03m in the library and from 1.6m to 1.45m in the retail store. B-PRP performs much better than RSSI with non-line-of-sight (NLoS) beacons. The median error for RSSI is 2.34m with NLoS beacons in the library compared to 1.63m with B-PRP.

B-PRP+RSSI: One might wonder if B-PRP can be augmented with RSSI to achieve even better performance. We augment B-PRP with RSSI to test this hypothesis. As shown in Figure 7, the method works approximately similar to B-PRP. As we demonstrate in the next subsection, this is because at smaller distances, RSSI experiences little packet loss and helps our model make better inference. However, at

Environment	B-PRP	B-PRP + RSSI	Bayesian RSSI [30]	Horus [57]	Bayesian FP [8]	MCL [18]
Library	1.03m	0.91m (↓ 11.6%)	1.3m (↑ 26.2%)	1.83m (↑ 77.6%)	1.93m (↑ 87.4%)	2.26m (↑ 119%)
Retail Store	1.45m	1.46m (↑ 0.6%)	2.05m (↑ 41.4%)	1.85m (↑ 27.6%)	1.95m (↑ 34.5%)	2.93m (↑ 102%)

TABLE 1: **Median error (in m) of B-PRP and baselines:** B-PRP performs best in both environments followed by Bayesian-RSSI in the library and Horus in retail store. Fusion of B-PRP and RSSI performs slightly better in the ideal library environment with many beacons at close distance. Horus and Bayesian FP underperform as they require more training states for better accuracy. All methods perform worst in the harsh retail environment.

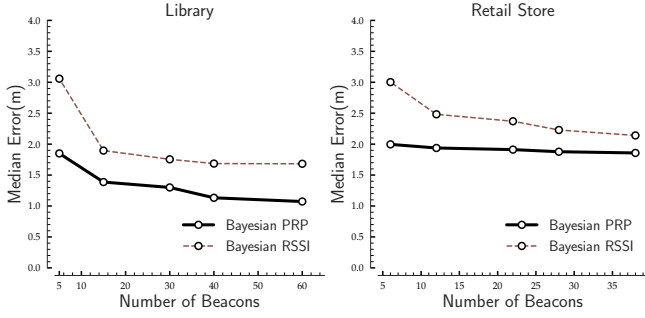


Fig. 8: Variation in median error for B-PRP with beacon number. The error is within $2m$ for all cases. With 5 beacons, B-PRP performance is better than Bayesian RSSI: 65% (library) and 50% (retail store).

large distances, RSSI experiences larger sampling bias and consequentially, just acts as noise, thereby hurting the model.

8.2 Beacon Number and Placement

We evaluate the robustness of B-PRP against the best performing baseline—Bayesian-RSSI to two factors—the number of beacons and the placement of beacons.

Beacon Number: We evaluated the accuracy with fewer number of beacons (lower bound is set to three beacons – the minimum required to localize). Lower number of beacons will reduce the localization infrastructure cost. In Figure 8, we see B-PRP performance degrades slowly than Bayesian-RSSI to decreasing beacon density. The median error of localization for B-PRP is always within $2m$. For Bayesian-RSSI, with lower beacons, the error is as high as $3m$. With 5 beacons, B-PRP performance is 65% better than Bayesian-RSSI in the library and 50% better in the retail store. Also, note that just with 5 beacons, B-PRP performs better or equal to Bayesian-RSSI with upto 60 beacons. This, yet again, demonstrates that the errors in RSSI-based positioning cannot be solved by just additional deployments, but are fundamental (sampling bias and multipath).

Beacon Placement: How does the placement of a beacon with respect to the receiver impact the localization accuracy by B-PRP and RSSI? If we use only beacons that are closer than $2m$ to the reception location, both PRP and RSSI errors are good (c.f. Table 2). RSSI performs slightly better in Line-of-Sight scenario due to the less variance in RSSI values and more distance information at very close range. Fusion of B-PRP and RSSI also yields lower errors. When beacon distances become greater than $2m$, RSSI errors dramatically increase due to variance in RSSI values caused by multi-path and sampling bias. In comparison, PRP errors are much lower in order of $1.53m$ and $2.07m$ when beacons are more than $6m$ away from the receiver. Errors in RSSI also cause fusion results

Line-Of-Sight Condition	distance < $2m$			$2m < \text{distance} < 6m$			distance > $6m$		
	B-PRP	RSSI	B-PRP + RSSI	B-PRP	RSSI	B-PRP + RSSI	B-PRP	RSSI	B-PRP + RSSI
LOS	0.89m	0.5m	0.5m	0.63m	3.57m	0.62m	1.53m	3.85m	1.56m
Non-LOS	0.85m	1.05m	0.57m	5m	5.95m	5.62m	2.07m	5.15m	2.7m

TABLE 2: Robustness To Beacon Placement: Recall, our median error using all beacons is $1.03m$. With only beacons that are closer than $2m$ to the receiver, both PRP and RSSI errors are low. Fusion of PRP and RSSI gives even lower errors of $0.5m$. In this range, RSSI values have less variance and more distance information. With beacons further than $2m$, RSSI variances increase which cause fusion results to be worse.

to be worse. Error for all approaches is high when we use only beacons, all of which are in a Non Line-of-Sight(NLOS) scenario and are at a distance between $2m$ and $6m$ from the receiver. This experiment highlights the importance of PRP. As RSSI estimates suffer from higher sampling bias with increasing distance, the underlying location information gets corrupted. This is why at larger distances, both Bayesian RSSI and B-PRP+RSSI do worse.

8.3 Evaluating Contact Tracing Distance Estimates

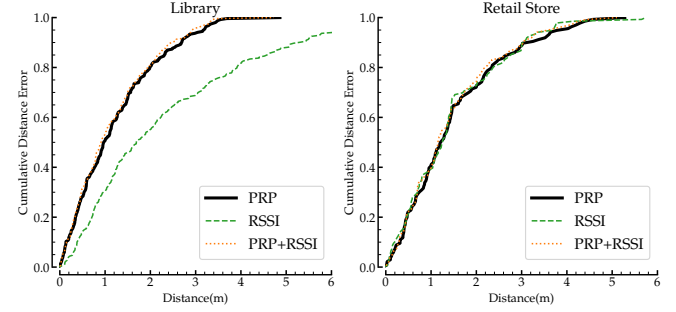


Fig. 9: CDF error distribution of contact tracing distance for PRP, RSSI and PRP+RSSI in library and retail store. PRP and PRP+RSSI gives the best median error in both environments.

We compare the accuracy of PRP against RSSI and PRP+RSSI in contact tracing distance estimation. We measure the absolute error between actual and estimated distances for each pair of person or receivers. We show cumulative distribution over errors in Figure 9.

PRP achieves a median distance error of $0.97m$ and $1.22m$ in the library and retail store. RSSI achieves distance errors of $1.69m$ and $1.25m$. PRP+RSSI performs the best with median distance errors of $0.91m$ and $1.15m$.

8.4 Minimizing beacon set-up cost

N_R	$b = 60$	$b = 6$	$b = 3$	$b = 1$
12	1.03	1.05	1.24	1.38
8	1.05	1.22	1.82	2.15
4	1.05	2.88	3.74	3.48

TABLE 3: B-PRP’s median localization error (in m) with varying number of known beacon locations b , and number of training locations N_R . Error increases as we decrease b (each row) and decrease N_R (each column). For $N_R = 12$, performance is almost same as with $b = 60$ and $b = 6$. Decreasing N_R impacts accuracy more than does b .

So far, we have used location information of all B beacons. Now, we will use the location information for only $b \ll B$

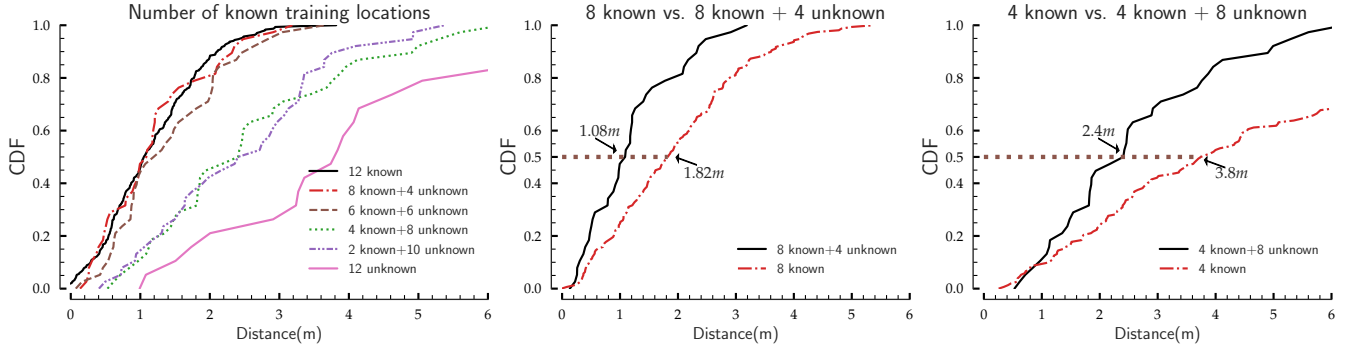


Fig. 10: **Reducing retraining efforts:** CDF for comparing errors of B-PRP when we train using data from some known and mostly unknown locations. If we have data from 12 known locations vs (6 known + 6 unknown) locations, we get the same accuracy level. In the right two subfigures, we show that we improved accuracy $\sim 40\%$ by adding data from unknown spots rather than only using data from known spots.

beacons. B is total number of beacons and b is the number of beacons with known location information. We use data to estimate $B - b$ unknown beacon locations. We then use these estimated values to track a receiver.

We vary the number of known beacon locations $b = \{1, 3, 6, 60\}$. $b = 60$ corresponds to when we know all beacon locations. We also vary the value of N_R i.e. the total number of training locations. Ideally, we would like to have less known beacons b and less training locations N_R . We show the results in Table 3.

We highlight three observations. *First*, when $(N_R = \{12, 8\})$ there is negligible difference in the CDF of the tracking errors between the cases of $b = 60$ and $b = 6$. *Second*, for any value of N_R , the errors increase when we decrease b , with the effects most pronounced for $N_R = 4$. *Finally*, the figures suggest that the effect of unknown beacon locations is *less significant* than the effect of the number of training locations. B-PRP can give the same level of performance with as low as $b = 3$ primary beacons when the number of training locations N_R is high. If we reduce N_R to 8, we need at least $b = 6$ known beacons.

These results highlight that B-PRP can be deployed for public spaces with little overhead. A retail store operator can just place beacons at random locations, and move around with a smartphone to some known locations. B-PRP can infer the beacon location on its own (for most beacons) and still achieve competitive performance.

8.5 Reducing training efforts

Till now, we have used the location information of all training spots N_R while training. Now, **let's use the information for only $r < N_R$ training spots** and estimate the remaining $N_R - r$ locations using our framework.

We change the value of known training locations $r = \{12, 8, 6, 4, 2, 0\}$, with $N_R = 12$. Figure 10 shows the results. In the leftmost sub-figure, we see that as r decreases, error increases; but notice that we can cut the known locations in half, from $r = 12$ to $r = 6$, without appreciable increase in error. This means that we can collect data from 12 spots but need to annotate only half of those and B-PRP can still maintain the same accuracy level. One might wonder, *do we really gain any performance improvement by adding data from unknown locations?* Figure 10 (two right sub-figures) validate

that conjecture. Suppose, our training dataset contains data from 12 training locations in total. Now, 8 of those are labeled with location information while 4 are unlabeled. If we train PRP parameters using only 8 labeled data locations, our median error from the trained model is $1.82m$. In contrast, if we use the entire dataset and treat the location of the 4 unlabeled data points as random variables in our framework, we improve the median error to $1.08m$. Similarly, if we have 4 labeled and 8 unlabeled locations, by using all the locations our errors improve from $3.8m$ to $2.4m$. Thus, data from unlabeled locations are valuable for training PRP parameters. This further eases the deployment cost by allowing operators to collect fewer labelled data points.

9 DISCUSSION AND LIMITATIONS

A few points are worth noting:

Applicability to general indoor environments: We design B-PRP with a focus on public indoor environments like retail stores that have stacked layouts. This layout is applicable to multiple spaces like libraries, warehouses, pharmacies, etc. and covers an important application area. While the current multipath-resilience model of B-PRP does not directly apply to other environments like homes, we believe PRP itself is applicable to such environments and provides the unique advantage of robustness at large distances. Furthermore, in such environments, obstacles like walls can be modelled using the approach followed in B-PRP.

Access to Layouts: We design the layout requirement for B-PRP to be low-effort. The layout and stacks can simply be extracted from the floorplan of the store, either manually or through an app. This makes the deployment effort low. Furthermore, B-PRP can apply to store layouts with more stacks than the ones used in this paper. We may encounter geometric elements like *three stacks away* ($3 - S$), *four stacks away* ($4 - S$) etc. We do not necessarily need a separate PRP function for each of these elements. Since PRP becomes very low after certain number of stacks, we can club these spaces into one geometric element and learn a single model.

Computational complexity: Bayesian MCMC techniques may take more time to infer location. We ran our computations in python on a MacBook Pro laptop with $2.5GHz$ Intel Core i7 processor and $16GB$ RAM. With 60 beacons, it took us ~ 3 seconds to find the next location, within our time

resolution ($\delta = 10\text{s}$) for localization. We can further speed-up by using native code and parallelizing the inference.

Scalability to the number of packets: One limitation of B-PRP is that it needs more than one packet to localize. We can reduce the number of packets used for localization by changing the advertising frequency. We observe in our experiments that as we lower the sending rate from 10Hz to 1Hz , while keeping the localization rate to once per 10 seconds, the median error increases by just 0.2m .

10 RELATED WORK

We can classify localization art on different factors—communication signal used for localization, models to relate distance and signal properties. Most works use signals exchanged with anchor nodes (known location) to infer location of target. Anchor nodes can be —WiFi access points [3], Bluetooth beacons [60, 52, 32], FM radios [9], Zigbee devices [27], ultra-wide band (UWB) devices [12], RFID tags [49, 56, 23, 22], ultra-sound emitters [19], light emitters [28, 26, 59, 61], 60GHz devices [34, 5], sub-centimeter sized devices [33]. In contrast, we use BLE beacons which offer advantages over the others. WiFi access points and cameras require continuous power and are more expensive than BLE beacons, which run on long-lasting batteries (lasting 3 to 5 years). A store can deploy hundreds of BLE beacons at a lower cost than WiFi access points or video cameras. We can scale BLE-based systems through past work in opportunistic listening that ensures better channel sharing [13]. WiFi, while widely available in public spaces such as malls and coffee shops, are often absent in large indoor retail stores (e.g., Walmart), in part because the presence of WiFi allows individuals in the store to comparison shop, putting the physical store at a competitive disadvantage. While [12] shows the promise of low-cost UWB sensing, the solution requires the widespread adoption of UWB tags to track objects. With BLE, we can track consumers via their Bluetooth enabled smartphones.

The localization techniques use different signal property — RSS or received signal strength [3, 10, 55], CSI or channel state information [45, 50], AoA or angle of arrival [54, 53, 25], ToF or time-of-flight [31, 42, 41]. AoA, ToF and CSI systems require hardware level changes on the receiver side and thus cannot be used by a retail store with customers who use commodity smartphones. Range free techniques use less accurate proximity information [18, 38, 15]. We use a new property—packet reception probability which is light weight and can be easily deployed on commercial smartphones.

Received Signal Strength (RSSI) systems are broadly of two types—model-based and fingerprint-based. Model-based techniques [30, 10, 4] represent RSSI loss between anchor and target as a function of distance. Fingerprint-based techniques [3], [57] build a map of probable RSS values from anchor nodes at sampled locations. Here we use a more robust property and design an easy-to-configure framework.

In this paper, we study tracking for public spaces like retail stores which have attracted attention due to proximity marketing [35]. Radhakrishnan et al. [36, 37] look at the problem of inferring item interaction in stores using wearable sensors. iBILL [52] jointly uses iBeacon RSSI model and inertial sensors to localize in supermarkets with 90% error less than 3.5m . Tagbooth [29], ShopMiner [43] tracks customer interaction with commodities using RFID tags in

retail stores. The closest approach to our work is [11] which counts packets to estimate distance. But here, we estimate using packet reception probability (PRP). We show PRP as a robust estimator of distance, and propose a Bayesian framework to estimate distance using PRP.

11 CONCLUSION

This paper establishes the feasibility of using Bluetooth Low-Energy (BLE) to provide a robust, scalable indoor localization solution using commodity hardware. Demonstrating the feasibility of BLE based distance estimation technique is particularly important during the current pandemic, where BLE has emerged as key technology for contact-tracing. BLE-based distance estimation today relies on either RSSI or just presence, both of which have publicly documented failure modes. We analyze the fundamental underpinnings of these failure modes and demonstrate robust localization through the Bayesian formulation of a new metric—Packet Reception Probability—that *exploits the absence of received packets*. We show significant improvements over the state of the art RSSI methods in two typical public spaces—a retail store and a library. We show that fusing B-PRP with RSSI is beneficial at short distances ($\leq 2\text{m}$). Beyond $\geq 2\text{m}$, fusion is worse than B-PRP, as RSSI based estimates beyond $\geq 2\text{m}$ are effectively de-correlated with distance. Our solution does not require any hardware, firmware, or driver-level changes to off-the-shelf devices, and involves minimal deployment and re-training costs. We have developed a triangle inequality based joint likelihood framework that directly estimates contact tracing distance between two individuals rather than estimating their locations first, which gives us 10% performance improvement. While our solution is the first step toward robust, reliable indoor contact tracing, we are extending our framework for peer-to-peer distance estimations without beacons (i.e. using only smartphones) for outdoor settings.

REFERENCES

- [1] 2014. Altbeacon. <https://github.com/AltBeacon/android-beacon-library-reference>. (2014).
- [2] R. Ayyalasomayajula, D. Vasisht, and D. Bharadia. 2018. Bloc: csi-based accurate localization for ble tags. In *ACM CoNEXT*.
- [3] P. Bahl and V. N. Padmanabhan. 2000. Radar: an in-building rf-based user location and tracking system. In *INFOCOM 2000*. Vol. 2. Ieee, 775–784.
- [4] N. Banerjee, S. Agarwal, P. Bahl, R. Chandra, A. Wolman, and M. Corner. 2010. Virtual compass: relative positioning to sense mobile social interactions. In *International Conference on Pervasive Computing*. Springer.
- [5] G. Bielsa, J. Palacios, A. Loch, D. Steinmetzer, P. Casari, and J. Widmer. 2018. Indoor localization using commercial off-the-shelf 60 ghz access points. In *2018 IEEE Conference on Computer Communications, INFOCOM 2018, Honolulu, HI, USA, April 16-19, 2018*, 2384–2392.
- [6] 2014. Blufi, bluetooth to wifi gateway. <http://bluvision.com/blufi/>. (2014).
- [7] D. Chen, K. G. Shin, Y. Jiang, and K.-H. Kim. 2017. Locating and tracking ble beacons with smartphones. In *Proceedings of the 13th International Conference on emerging Networking Experiments and Technologies*.

- [8] L. Chen, L. Pei, H. Kuusniemi, Y. Chen, T. Kröger, and R. Chen. 2013. Bayesian fusion for indoor positioning using bluetooth fingerprints. *Wireless personal communications*, 70, 4, 1735–1745.
- [9] Y. Chen, D. Lymberopoulos, J. Liu, and B. Priyantha. 2012. Fm-based indoor localization. In *MobiSys*. ACM.
- [10] K. Chintalapudi, A. Iyer, and V. Padmanabhan. 2010. Indoor localization without the pain. In *MobiCom*.
- [11] S. De, S. Chowdhary, A. Shirke, Y. L. Lo, R. Kravets, and H. Sundaram. 2017. Finding by counting: a probabilistic packet count model for indoor localization in ble environments. In *Proceedings of the 11th Workshop on Wireless Network Testbeds, Experimental evaluation & Characterization*. ACM, 67–74.
- [12] B. Großwindhager, M. Rath, J. Kulmer, M. S. Bakr, C. A. Boano, K. Witrals, and K. Römer. 2018. Salma: uwb-based single-anchor localization system using multipath assistance. In *Proceedings of the 16th ACM Conference on Embedded Networked Sensor Systems*. ACM.
- [13] A. F. Harris III, V. Khanna, G. Tuncay, R. Want, and R. Kravets. 2016. Bluetooth low energy in dense iot environments. *IEEE Communications Magazine*, 54, 12.
- [14] S. He and S.-H. G. Chan. 2016. Wi-fi fingerprint-based indoor positioning: recent advances and comparisons. *IEEE Communications Surveys & Tutorials*, 18, 1, 466–490.
- [15] T. He, C. Huang, B. M. Blum, J. A. Stankovic, and T. Abdelzaher. 2003. Range-free localization schemes for large scale sensor networks. In *Proceedings of the 9th annual international conference on Mobile computing and networking*. ACM, 81–95.
- [16] K. Heurtefeux and F. Valois. 2012. Is rssi a good choice for localization in wireless sensor network? In *AINA, 2012 IEEE 26th International Conference on*. IEEE.
- [17] M. D. Hoffman and A. Gelman. 2014. The no-u-turn sampler: adaptively setting path lengths in hamiltonian monte carlo. *Journal of Machine Learning Research*, 15, 1.
- [18] L. Hu and D. Evans. 2004. Localization for mobile sensor networks. In *Proceedings of the 10th annual international conference on Mobile computing and networking*.
- [19] W. Huang, Y. Xiong, X.-Y. Li, H. Lin, X. Mao, P. Yang, and Y. Liu. 2014. Shake and walk: acoustic direction finding and fine-grained indoor localization using smartphones. In *INFOCOM, 2014 Proceedings IEEE*. IEEE, 370–378.
- [20] 2015. Ibeek. <http://bluvision.com/ibeek-5/>. (2015).
- [21] 2003. Iperf. <https://iperf.fr>. (2003).
- [22] C. Jiang, Y. He, S. Yang, J. Guo, and Y. Liu. 2019. 3d-omnitrack: 3d tracking with COTS RFID systems. In *Proceedings of the 18th International Conference on Information Processing in Sensor Networks, IPSN 2019, Montreal, QC, Canada, April 16-18, 2019*, 25–36.
- [23] C. Jiang, Y. He, X. Zheng, and Y. Liu. 2018. Orientation-aware rfid tracking with centimeter-level accuracy. In *Proceedings of the 17th ACM/IEEE International Conference on Information Processing in Sensor Networks*. IEEE Press, 290–301.
- [24] M. Kotaru, K. Joshi, D. Bharadia, and S. Katti. 2015. Spotfi: decimeter level localization using wifi. In *ACM SIGCOMM Computer Communication Review* number 4. Vol. 45. ACM, 269–282.
- [25] S. Kumar, S. Gil, D. Katabi, and D. Rus. 2014. Accurate indoor localization with zero start-up cost. In *Proceedings of the 20th annual international conference on Mobile computing and networking*. ACM, 483–494.
- [26] Y.-S. Kuo, P. Pannuto, K.-J. Hsiao, and P. Dutta. 2014. Luxapose: indoor positioning with mobile phones and visible light. In *MobiCom*. ACM, 447–458.
- [27] S.-Y. Lau, T.-H. Lin, T.-Y. Huang, I.-H. Ng, and P. Huang. 2009. A measurement study of zigbee-based indoor localization systems under rf interference. In *Proceedings of the 4th ACM international workshop on Experimental evaluation and characterization*. ACM.
- [28] S. Liu and T. He. 2017. Smartlight: light-weight 3d indoor localization using a single led lamp. In *SenSys*.
- [29] T. Liu, L. Yang, X.-Y. Li, H. Huang, and Y. Liu. 2015. Tagbooth: deep shopping data acquisition powered by rfid tags. In *Computer Communications (INFOCOM), 2015 IEEE Conference on*. IEEE, 1670–1678.
- [30] D. Madigan, E. Einahrawy, R. P. Martin, W.-H. Ju, P. Krishnan, and A. Krishnakumar. 2005. Bayesian indoor positioning systems. In *INFOCOM 2005. Vol. 2. IEEE*, 1217–1227.
- [31] A. T. Mariakakis, S. Sen, J. Lee, and K.-H. Kim. 2014. Sail: single access point-based indoor localization. In *MobiSys*. ACM, 315–328.
- [32] A. Montanari, S. Nawaz, C. Mascolo, and K. Sailer. 2017. A study of bluetooth low energy performance for human proximity detection in the workplace. In *Pervasive Computing and Communications (PerCom), 2017 IEEE International Conference on*. IEEE, 90–99.
- [33] R. Nandakumar, V. Iyer, and S. Gollakota. 2018. 3d localization for sub-centimeter sized devices. In *Proceedings of the 16th ACM Conference on Embedded Networked Sensor Systems, SenSys 2018, Shenzhen, China, November 4-7, 2018*, 108–119.
- [34] J. Palacios, G. Bielsa, P. Casari, and J. Widmer. 2019. Single- and multiple-access point indoor localization for millimeter-wave networks. *IEEE Trans. Wireless Communications*, 18, 3, 1927–1942.
- [35] 2017. Proximity marketing in retail. <https://www.proximity.directory/reports/>. (2017).
- [36] M. Radhakrishnan, S. Eswaran, A. Misra, D. Chander, and K. Dasgupta. 2016. Iris: tapping wearable sensing to capture in-store retail insights on shoppers.
- [37] M. Radhakrishnan, S. Sen, V. Subbaraju, A. Misra, and R. Balan. 2016. Iot+ small data: transforming in-store shopping analytics and services.
- [38] M. Rudafshani and S. Datta. 2007. Localization in wireless sensor networks. In *IPSN 2007. 6th International Symposium on*. IEEE, 51–60.
- [39] J. Salvatier, T. V. Wiecki, and C. Fonnesbeck. 2016. Probabilistic programming in python using pymc3. *PeerJ Computer Science*, 2, e55.
- [40] M. Schulz, J. Link, F. Gringoli, and M. Hollick. 2018. Shadow wi-fi: teaching smartphones to transmit raw signals and to extract channel state information to implement practical covert channels over wi-fi. In *Proceedings of the 16th Annual International Conference on Mobile Systems, Applications, and Services*, 256–268.
- [41] S. Sen, D. Kim, S. Laroche, K.-H. Kim, and J. Lee. 2015. Bringing cupid indoor positioning system to practice.

- In WWW. International World Wide Web Conferences Steering Committee, 938–948.
- [42] S. Sen, J. Lee, K.-H. Kim, and P. Congdon. 2013. Avoiding multipath to revive inbuilding wifi localization. In *Proceeding of the 11th annual international conference on Mobile systems, applications, and services*. ACM, 249–262.
 - [43] L. Shangguan, Z. Zhou, X. Zheng, L. Yang, Y. Liu, and J. Han. 2015. Shopminer: mining customer shopping behavior in physical clothing stores with cots rfid devices. In *Proceedings of the 13th ACM conference on embedded networked sensor systems*. ACM, 113–125.
 - [44] X. Tian, M. Wang, W. Li, B. Jiang, D. Xu, X. Wang, and J. Xu. 2018. Improve accuracy of fingerprinting localization with temporal correlation of the rss. *IEEE Transactions on Mobile Computing*, 17, 1, 113–126.
 - [45] X. Tian, S. Zhu, S. Xiong, B. Jiang, Y. Yang, and X. Wang. 2018. Performance analysis of wi-fi indoor localization with channel state information. *IEEE Transactions on Mobile Computing*.
 - [46] N. Van Doremalen et al. 2020. Aerosol and surface stability of sars-cov-2 as compared with sars-cov-1. *New England Journal of Medicine*, 382, 16, 1564–1567.
 - [47] D. Vasisht, A. Jain, C.-Y. Hsu, Z. Kabelac, and D. Katabi. 2018. Duet: estimating user position and identity in smart homes using intermittent and incomplete rf-data. *Proceedings of the ACM on Interactive, Mobile, Wearable and Ubiquitous Technologies*, 2, 2, 84.
 - [48] D. Vasisht, S. Kumar, and D. Katabi. 2016. Decimeter-level localization with a single wifi access point. In *NSDI*. Vol. 16, 165–178.
 - [49] J. Wang and D. Katabi. 2013. Dude, where’s my card?: rfid positioning that works with multipath and non-line of sight. In *ACM SIGCOMM Computer Communication Review* number 4. Vol. 43. ACM, 51–62.
 - [50] Y. Wang, J. Liu, Y. Chen, M. Gruteser, J. Yang, and H. Liu. 2014. E-eyes: device-free location-oriented activity identification using fine-grained wifi signatures. In *Proceedings of the 20th annual international conference on Mobile computing and networking*. ACM, 617–628.
 - [51] Y. Wen, X. Tian, X. Wang, and S. Lu. 2015. Fundamental limits of rss fingerprinting based indoor localization. In *Computer Communications (INFOCOM), 2015 IEEE Conference on*. IEEE, 2479–2487.
 - [52] X. Wu, R. Shen, L. Fu, X. Tian, P. Liu, and X. Wang. 2017. Ibill: using ibeacon and inertial sensors for accurate indoor localization in large open areas. *IEEE Access*, 5.
 - [53] J. Xiong and K. Jamieson. 2013. Arraytrack: a fine-grained indoor location system. In *Usenix*.
 - [54] J. Xiong and K. Jamieson. 2010. Secureangle: improving wireless security using angle-of-arrival information. In *Proceedings of the 9th ACM SIGCOMM Workshop on Hot Topics in Networks*. ACM, 11.
 - [55] J. Yang and Y. Chen. 2009. Indoor localization using improved rss-based lateration methods. In *GLOBECOM 2009-2009 IEEE Global Telecommunications Conference*. IEEE, 1–6.
 - [56] L. Yang, J. Cao, W. Zhu, and S. Tang. 2015. Accurate and efficient object tracking based on passive rfid. *IEEE Transactions on Mobile Computing*, 14, 11, 2188–2200.
 - [57] M. Youssef and A. Agrawala. 2005. The horus wlan location determination system. In *MobiSys*. ACM.
 - [58] A. Zanella. 2016. Best practice in rss measurements and ranging. *IEEE Communications Surveys & Tutorials*, 18, 4, 2662–2686.
 - [59] C. Zhang and X. Zhang. 2017. Pulsar: towards ubiquitous visible light localization. In *Proceedings of the 23rd Annual International Conference on Mobile Computing and Networking*. ACM, 208–221.
 - [60] X. Zhao, Z. Xiao, A. Markham, N. Trigoni, and Y. Ren. 2014. Does btle measure up against wifi? a comparison of indoor location performance. In *European Wireless*.
 - [61] S. Zhu and X. Zhang. 2017. Enabling high-precision visible light localization in today’s buildings. In *Proceedings of the 15th Annual International Conference on Mobile Systems, Applications, and Services*. ACM, 96–108.